J Mol Model (2015) 21:56
DOI 10.1007/s00894-015-2605-5

ORIGINAL PAPER

The structure of adsorbed cyclic chains

Aleksander Kuriata · Andrzej Sikorski

Received: 14 November 2014 / Accepted: 1 February 2015

Abstract In order to determine the structure of polymer films formed of cyclic chains (rings) we developed and studied a simple coarse-grained model. Our main goal was to check how the percolation and jamming thresholds in such a system were related to the thresholds obtained for linear flexible chains system, i.e., how the geometry of objects influenced both thresholds. All atomic details were suppressed and polymers were represented as a sequence of identical beads and the chains were embedded to a square lattice (a strictly 2D model). The system was athermal and the excluded volume was the only potential introduced. A random sequential adsorption algorithm was chosen to determine the properties of a polymer monolayer. It was shown that the percolation threshold of cyclic chains was considerably higher than those of linear flexible chains while the jamming thresholds for both chain architectures are very similar. The shape of adsorbed cyclic chains was found to be more prolate when compared to average single chain.

Keywords Cyclic polymers · Jamming · Lattice models · Percolation · Random Sequential Adsorption

Introduction

Cyclic polymers have attracted the attention of researchers for many years [1, 2]. The loop closure makes the chain's architecture different from a linear one and causes differences in the static and dynamic properties. The structure of cyclic chains and their dynamic properties were subjects of numerous experimental [3–8], theoretical [9–11], and simulation [12–24] studies although the discussion about their size and viscoelastic properties is not closed yet. The introduction of an adsorbing surface into a polymeric system dramatically changes the properties of these systems [25]. The simulations of adsorbed macromolecules are rather numerous and these studies were mainly devoted to the distribution of polymer segments and the behavior of such structural elements like trains, loops, and tails. One has to remember that these models were quasi-two-dimensional whith three-dimensional polymer chains strongly adsorbed. Models of strictly two-dimensional chains were also studied, but the question concerning if the percolation and the jamming (the maximum coverage of the substrate by the objects) in systems with ring macromolecules was raised only once [26]. Percolation is a process in which the system under consideration spans infinitely. In finite systems the percolation occurs when a cluster formed of sites occupied by objects approaches the size of the space, i.e., it spans from one border of the system to the opposite one. The percolation phenomena were extensively studied theoretically but, in spite of this effort, there are still many problems that are far from being understood especially for larger and irregular objects like polymer chains [27].

The theoretical studies of the percolation in a film formed from long polymer chains were limited to computer simulation studies. The percolation in polymer systems on solid surfaces was mainly studied using the random sequential adsorption (RSA) algorithm [28–35]. In this method the polymer chains were randomly deposited on the flat substrate. The deposited chains were immobilized, thus, the adsorption was irreversible. The objects could not cross themselves, i.e., the excluded volume was introduced into the model. The percolation and jamming thresholds can be determined directly by these means. The most popular objects studied using the RSA

This paper belongs to Topical Collection 6th conference on Modeling & Design of Molecular Materials in Kudowa Zdrój (MDMM 2014)

A. Kuriata · A. Sikorski (✉)
Department of Chemistry, University of Warsaw, Pasteura 1, 02-093 Warsaw, Poland
e-mail: sikorski@chem.uw.edu.pl

Published online: 21 February 2015

method were stiff rods (needles) but some results, especially the scaling properties of the both thresholds are still contradictory [28–32, 36–42]. The other objects were ellipses [43, 44] or rectangles [45, 46] where the percolation depends strongly on their aspect ratio. Short flexible and semi-flexible chains were also studied by means of the RSA method and it was shown that the percolation threshold in the case of flexible chain decreases with the increase of the chain length while for semi-flexible chains its changes were non-monotonous [28, 47–54]. In another recent study the RSA method was applied for some different macromolecular architectures [33]. This work showed that the influence of the chain architecture (number of branches in a star polymer) on the percolation and jamming thresholds was surprisingly weak. The cooperative motion algorithm (CMA) was also applied for studies of the percolation in two-dimensional lattice polymer-solvent systems [55]. It was shown that the percolation threshold did not simply scale with the local chain density and two scalings regimes could be identified here. The cross-overs between these regimes corresponded to rapid changes of structural polymer properties and thus, to the changes of chains' fractal dimension. It should be noted that the scaling theory of de Gennes predicts that polymer concentration φ^* at which the transition between dilute and semi-dilute regimes occurs depends linearly on the local density in two-dimensional systems [56].

In this work we studied the RSA-type model of polymer chain adsorption on a planar and homogenous surface. The model polymer chains were represented by the sequences of beads and their positions were restricted to vertices of a square lattice. The cyclic chains were randomly put on the substrate and immobilized while the properties of the chains in the formed film were determined. The paper is organized as follows: in the next section *The model and the simulation algorithm* we described the model and the simulation method. In the section *Results and discussion* the results were presented and compared to other macromolecular architectures and to theoretical considerations. The section *Conclusions* contains the most important conclusions concerning our results with comparison to other macromolecular systems.

The model and the simulation algorithm

The coarse-grained model of macromolecules was realized by the construction of cyclic sequences of N identical beads, where a single bead represented some chemical mers. This simple model was found to be sufficient for the studies of properties of a chain as a whole [57]. In order to make the calculations more efficient we have also introduced a lattice approximation: the positions of polymer beads in space were limited to vertices of a square lattice. The excluded volume was the only potential introduced into the model and thus, chains could not cross themselves. Other long-distance interactions were assumed to be identical and, hence, the system was athermal and the polymer chains were studied at good solvent conditions. Our system was a square of the edge L which represented a substrate with $L \times L$ points on which the polymer chains were adsorbed. The RSA was realized in the following way [55]. The chains were picked at random from a pool, placed onto the substrate and then they were immobilized: no diffusion of the entire macromolecules and no conformational changes were allowed. The adsorbed chains could not overlap themselves – it was realized by the forbidding the double occupancy of lattice points by polymer beads. Periodic boundary conditions were imposed in both directions on the system studied. Before the RSA process was performed a library containing a collection of the chains conformations of a given length N had been prepared [55]. For shorter chains the libraries were filled with all possible conformations. For longer chains the libraries were filled up with 10^7 different representative conformations obtained in simulations. The algorithm, which generated these conformations, was based on the concept of Verdier-Stockmayer, i.e., local modifications of chain conformations were used [56–58]. Simulation started with the empty substrate. First, we chose randomly a location where the adsorbed chain would start. If this lattice point was empty, we selected at random one of the chain conformations from our library. Then, we checked lattice sites of the substrate for this conformation. If these sites were empty a new chain was added to the system, otherwise the entire procedure was repeated. After each chain was added we checked if the percolation cluster was already formed. The RSA method enables one to study the case of strong and irreversible adsorption of objects [59]. A tree-based union/find efficient algorithm invented by Neman and Ziff was employed to keep track of cluster connectivity [60]. After the percolation threshold was reached the RSA procedure was continued until the jamming occurred. Based on our previous findings described in detail in ref. [28] we assumed that the jamming occurred if at least $5 \times 10^3 \times L^2$ unsuccessful attempts of adding a new chain were made. In order to assure the correct values we performed from 10^4 (for short chains $N < 20$) to 10^2 (for long chains) independent RSA procedures and the results were averaged over these runs.

Results and discussion

The simulations were performed for cyclic chains consisted of N=4 to N=100. The RSA method was found unable to study longer chains especially near the jamming threshold in such systems [49, 54]. The edge of the square substrate was

changed between $L=100$ and $L=2500$ lattice units. The finite size scaling procedure was done in order to obtain threshold values for an infinite size of the system [35, 50, 59]:

$$\left|c_p(L)-c_p(\infty)\right| \sim L^{-1/\nu}, \quad (1)$$

where $c_p(L)$ and $c_p(\infty)$ are the percolation thresholds for the Monte Carlo box $L\times L$ and for an infinite system respectively while ν is a universal critical exponent ($\nu=4/3$) [26]. Figure 1 presents the calculated values of c_p versus $(L/N)^{-1/\nu}$. All presented curves are linear and the extrapolation of percolation thresholds towards an infinite system can be made according to Eq. (1). The corrections to the thresholds obtained from simulations in a large system 2000×2000 are of order of 10^{-3}, which was below the standard error of these quantities. In the case of two-dimensional cyclic chains one can consider two definitions of the polymer concentration:

1. The ratio of the number of polymer beads (n chains each consisting of N beads) to the total number of sites in the system, i.e., we consider the chain's contour only:

$$\varphi_1 = {}^{nN}/_{L^2}. \quad (2)$$

2. The ratio of the total area covered by chains (contour plus area surrounded by the chain, i.e. the excluded area A_i) to the total number of sites in the system:

$$\varphi_2 = \sum_{i=1}^{n} A_i/L^2. \quad (3)$$

Figure 2 presents changes of the percolation threshold c_p for cyclic chains with the chain length N. For the sake of comparison the results concerning the linear flexible (acyclic) chains and stiff chains (needles) taken from ref. [28] were also added to this figure. In order to compare the results to flexible acyclic chains and needles the density of ring macromolecules was calculated according to Eq. (2). The flexible linear chains behave in the same way as was found in other simulations [50, 51]. The threshold for rings was found considerably higher than that for flexible chains in the entire range of the chain lengths what was expected as ring chains are smaller and more spherical than unbranched flexible chains of the same length and their perimeter is less jagged. The threshold for cyclic chains decreases with N in the entire range of the chain length with the exception for very short chains consisted of $N=4$ and $N=6$ beads. The behavior of these small objects is generally different than that of larger objects (see below), as they are simply stiff squares and rectangles respectively. The needles' behavior is different: initially the percolation threshold decreases when the size of the objects increases and then starts to increase slightly which was also observed in other simulations [32, 33, 38, 39]. It can be explained by the formation of local highly ordered blocks for longer objects: in spite of the high polymer concentration there is still unoccupied area available and the size of this area is comparable with the length of the needle [28, 31]. The possibility of the insertion of irregular objects like flexible acyclic and cyclic chains has to be considerably smaller than for needles.

The next parameter studied describing the film formed of adsorbed chains is the jamming threshold. This threshold can be determined analytically for one-dimensional systems only. The plot of the jamming threshold c_j for cyclic chains as the function of the chain length N is presented in Fig. 3. Values of

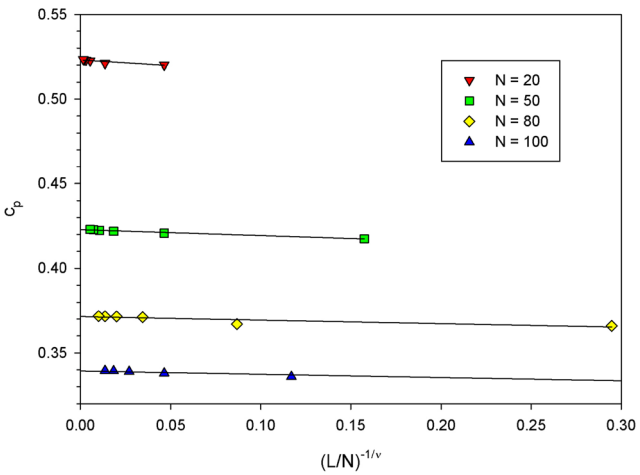

Fig. 1 The percolation thresholds c_p of rings as a function of $(L/N)^{-1/\nu}$. The chain lengths are given in the legend

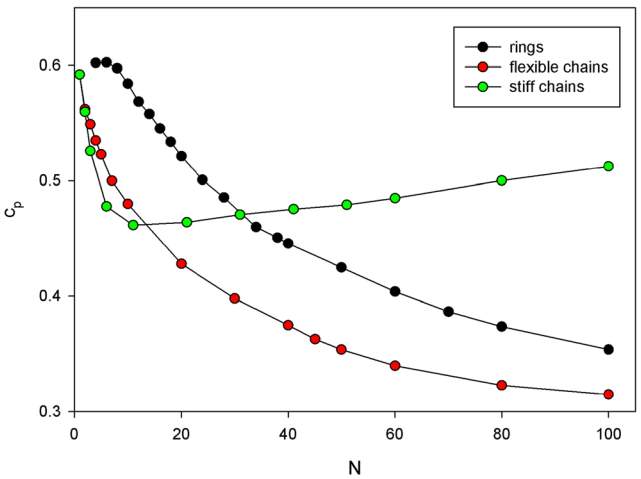

Fig. 2 The percolation threshold c_p as a function of the chain length N. The types of the objects used in the RSA procedure are given in the legend

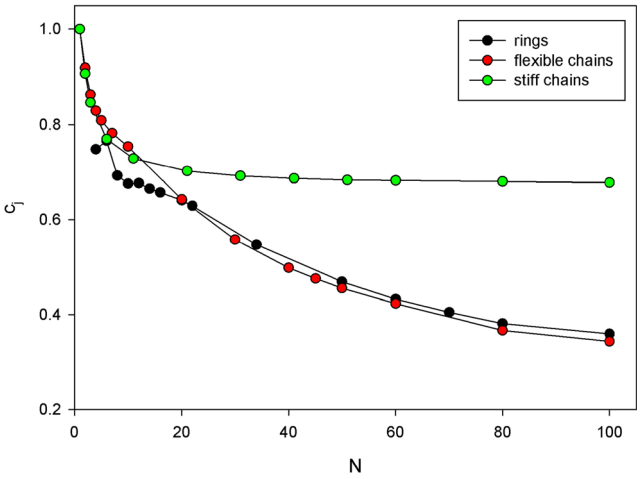

Fig. 3 The jamming threshold c_j as a function of the chain length N. The types of the objects used in the RSA procedure are given in the legend

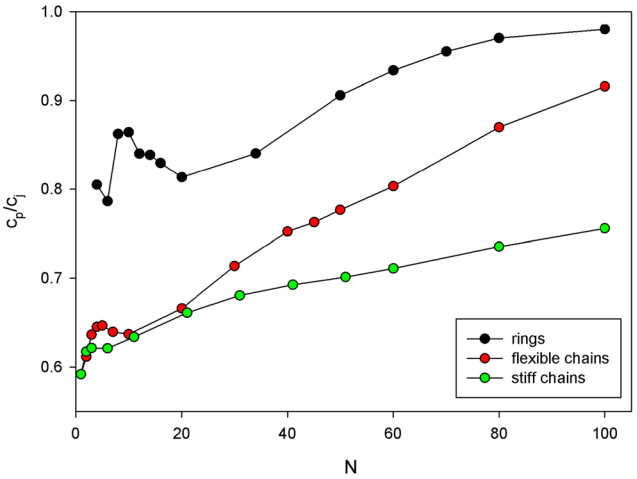

Fig. 4 Plot of the c_p/c_j ratio as a function of the chain length N. The types of the objects used in the RSA procedure are given in the legend

this threshold for flexible acyclic chains and needles were added to this figure for the sake of comparison. The plots for flexible acyclic and cyclic chains were very similar for longer chains $N>20$ although the threshold values for rings are slightly larger. Both jamming thresholds smoothly decrease in this chain length range. The threshold for unbranched flexible chains is monotonous for all chain systems under consideration with faster decrease for short chains while that for cyclic chains is smaller and non-monotonous in this region. The reason of this behavior is the same as mentioned above, i.e., the influence of the lattice approximation. For short chains the jamming threshold of needles and acyclic flexible polymers are very similar while the latter remains almost constant for larger values of N. Thus, the decrease of the jamming threshold with the chain length for flexible acyclic and cyclic chains is considerably faster than for needles. This decrease is also faster than suggested for short objects $N^{-0.19}$ (needles) and $N^{-0.17}$ (acyclic flexible chains) [29–31, 36].

The ratios c_p/c_j for flexible cyclic and acyclic chains as functions of the chain length N are presented in Fig. 4. The c_p/c_j curves for flexible chains show the increase of this ratio with the increasing chain length for $N>20$. For flexible acyclic and cyclic chains one can see a local maximum on the curve near $N=5$ and $N=10$ respectively which is a result of the lattice model used. For both chains architectures c_p/c_j ratios seems to approach the unity asymptotically. In other words, not many chains could be added to the system after the percolation was reached but one has to remember that for longer chains sometimes the jamming occurred before the percolation. The c_p/c_j ratio for needles also exhibits a maximum at $N=3$ and increases considerably slower approaching values close to 3/4. It results from extra packing ability of stiff linear chains: local ordered clusters of needles were formed [28]. The behavior of this ratio for needles is exactly the same as for the anisotropic case in ref. [42] and thus, it also does not confirm the hypothesis of Vandewalle et al. that it is constant [31]. If one assumes that in this case the ratio can be approximated by the formula $c_p/c_j=b\times\log(N)+c$ the value of constant is $b=0.123\pm0.003$ while Tarasevich et al. [42] found $b=0.119\pm0.003$. Flexible linear and cyclic chains do not exhibit such behavior: the ratio increases faster for the first ones and slower for the latter.

Figure 5 presents the same results as in Figs. 2 and 3 for cyclic chains but the interior (exclude) area of rings was also included, i.e., the polymer concentration on the substrate was determined according to Eq. (3). In this figure we also present jamming thresholds determined for squares taken from refs. [31, 62] and [63]. With the exception of the shortest chains ($N<10$) the behavior of c_p is quite different: it increases slightly

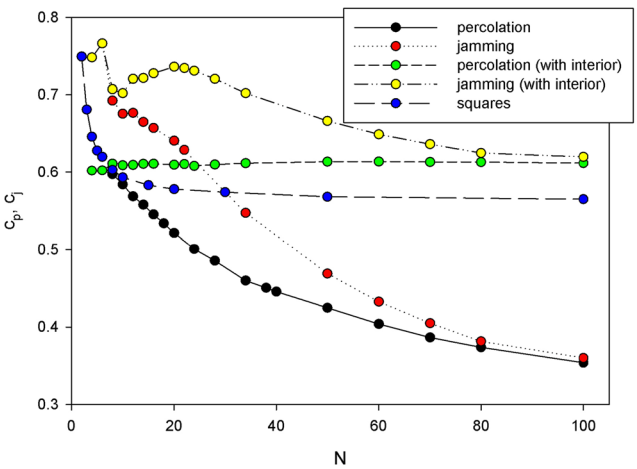

Fig. 5 The percolation threshold c_p and jamming threshold c_j as functions the chain length N. The polymer concentration was calculated according to Eq. (3). The types of the objects used in the RSA procedure are given in the legend

with the increase of the chain length. It should be pointed out that for cyclic polymers in the most cases, the percolation occurred before jamming contrary to blocks (squares) [31, 61, 62]. The jamming threshold of filled rings behave non-monotonously for $N<20$ and for longer chains it decreases with N. The jamming thresholds of filled rings are in this region larger than those of squares what means that irregular objects are able to fill the space better.

The structure of a polymer monolayer on the substrate can be clearly visible on snapshots of the system. Typical

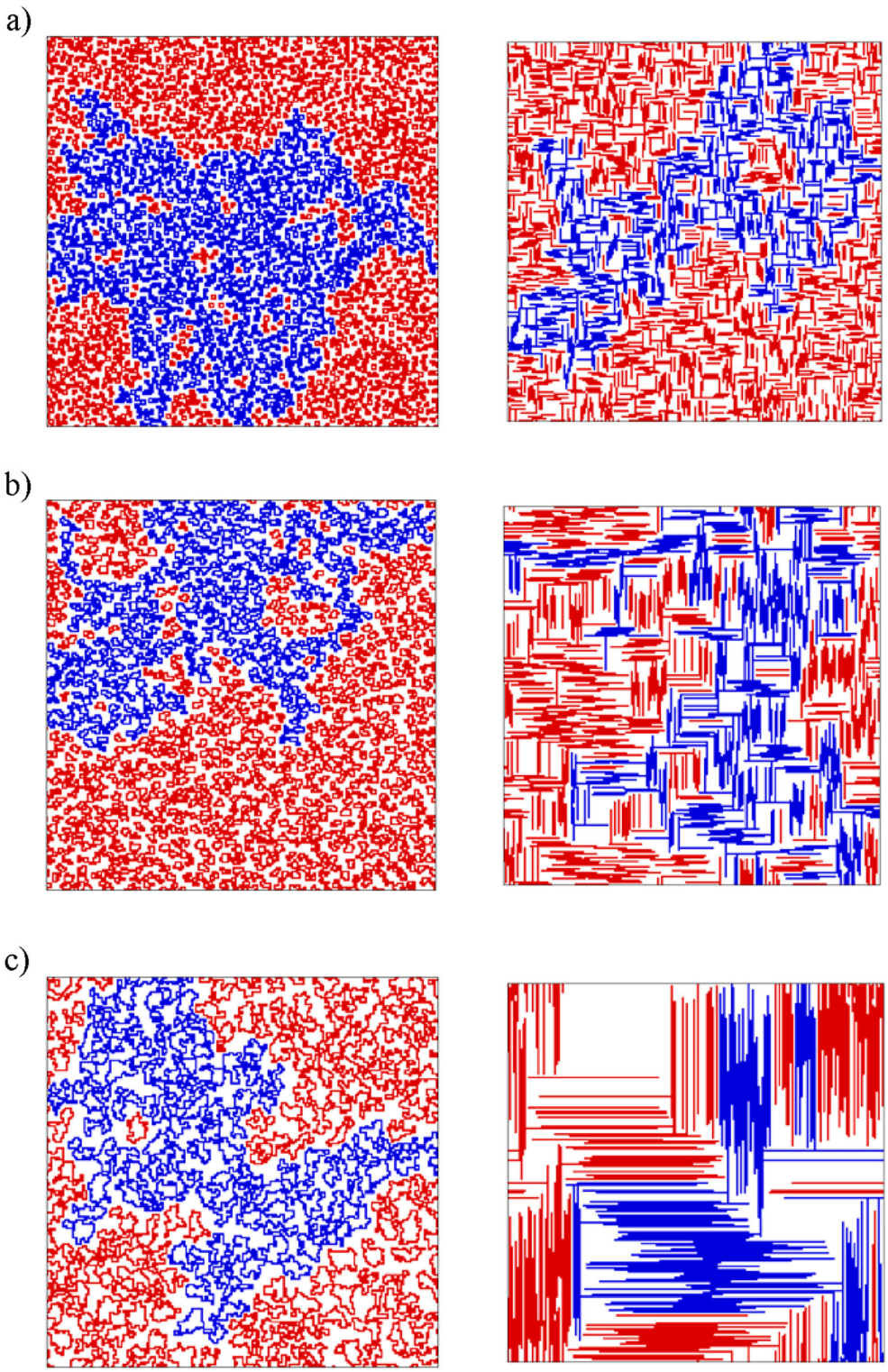

Fig. 6 Snapshots of the system at the percolation threshold for rings (left) and needles (right). The case of chain consisted of $N=8$ (**a**), $N=18$ (**b**), and $N=70$ (**c**) beads. The percolation cluster is marked in red

snapshots showing the systems consisting of short (N=8), intermediate (N=18), and long (N=70) chains near the percolation threshold are shown in Fig. 6. Figure 7 presents snapshots of the same systems near the jamming threshold. Snapshots of needles were also included into Figs. 6 and 7 for the sake of comparison. The structure of polymer films shown in the snapshots is generally consistent with the above-discussed changes of both thresholds with the object length. For both species one can see the decrease of thresholds with the increasing number of beads and the considerably lower thresholds for needles when comparing large objects. The main difference between systems with rings and needles at both thresholds is a local ordering of the latter.

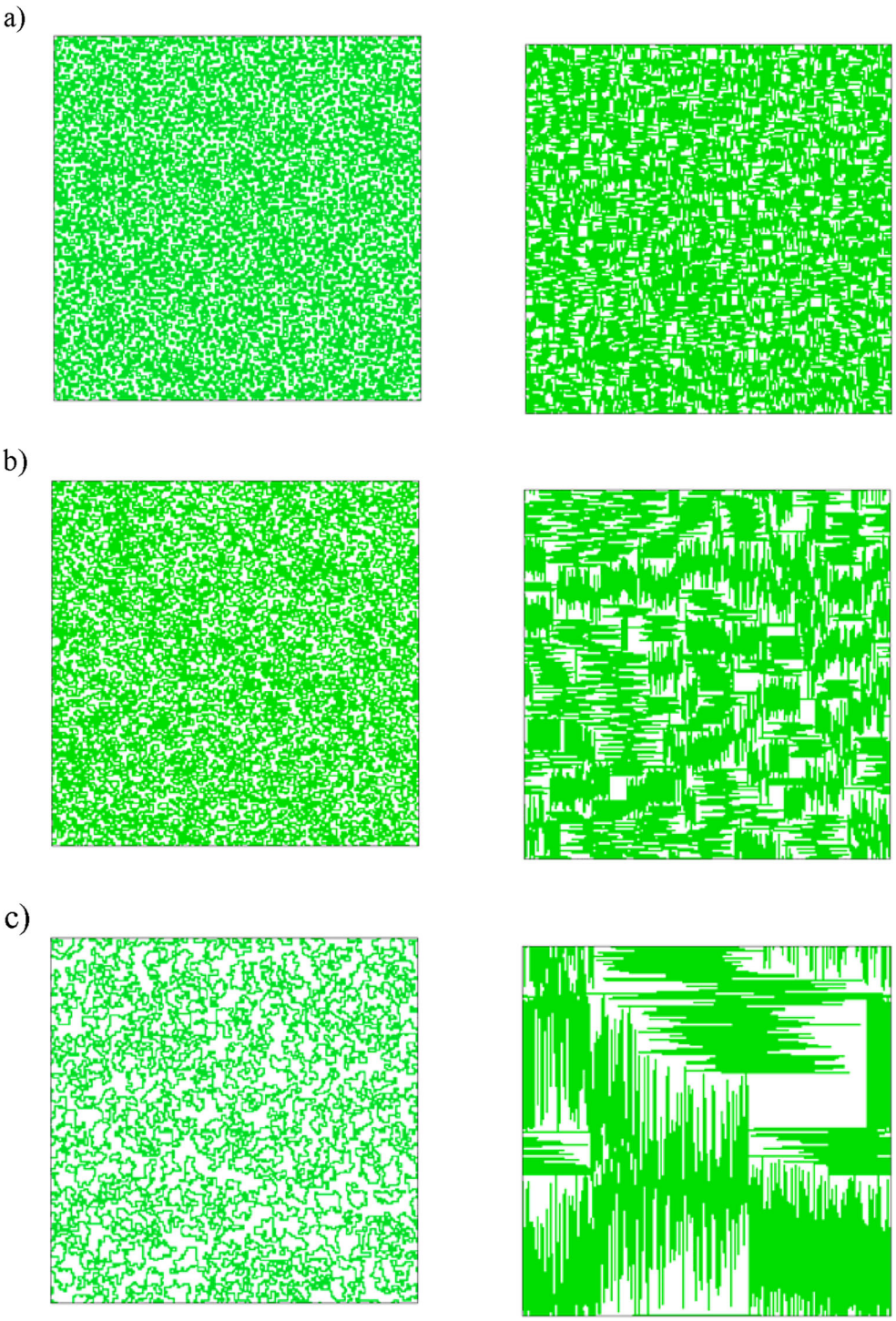

Fig. 7 Snapshots of the system at the jamming threshold for rings (left) and needles (right). The case of chain consisted of N=8 (**a**), N=18 (**b**), and N=70 (**c**) beads

The size of a polymer chain is usually described by the mean-squared radius of gyration $< S^2 >$ calculated as:

$$\langle S^2 \rangle = \frac{1}{N}\sum_{i=1}^{N}\left\langle (\mathbf{r}_i - \mathbf{r}_{CM})^2 \right\rangle, \quad (4)$$

where $\boldsymbol{r}_i$ is a vector denoting a position of an ith bead and $\mathbf{r}_{CM}$ denotes the position of the chain's center-of-mass position. The second parameter studied was the mean-squared diameter

$$\langle R^2 \rangle = \left\langle (\mathbf{r}_1 - \mathbf{r}_{N/2})^2 \right\rangle. \quad (5)$$

These size parameters are plotted in Fig. 8 as a function of the chain length in the log-log scale. With the exception of short chains (N<20) one can observe the scaling behavior of these parameters as N^{γ}. The scaling exponent was found to be 1.494 ±0.005 for$<R^2>$and 1.477±0.006 for$<S^2>$which is close to the theoretical value 3/2 and to other computer simulation results 1.52 and 1.494 for R^2 and S^2 respectively [12]. It has to be remembered that this is the exponent characteristic for single chains (diluted solutions) which is obvious as our adsorbed chains were produced as conformations that were characteristic for diluted solutions; in dense 2-dimensianal melts this exponent approaches the value 1 [48, 63]. A quite different behavior of polymer's size for N≤20 is caused by a short chain effect and by the lattice approximation. The latter introduced even large fluctuations of the mean-square radius of gyration for very short chains, which are very stiff: a ring consisting of N=4 beads appears in one conformation only as a square, the ring with N=6 beads forms one conformation too (a rectangle) occurring in two orientations and ring with N=8 beads is the first one that occurs in two different conformations.

The next problem under consideration concerned the shape of adsorbed chains. In order to study the instantaneous shape

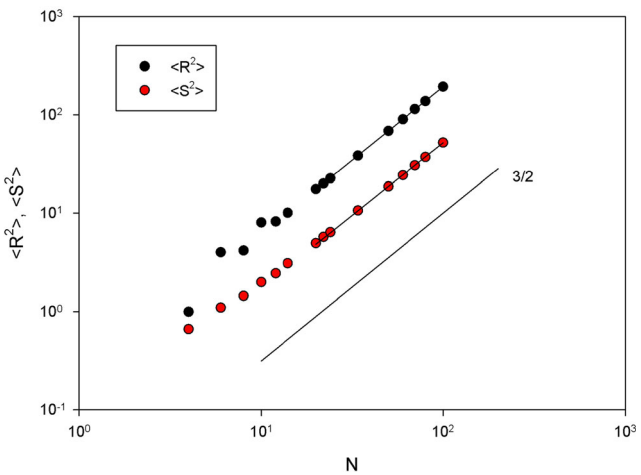

Fig. 8 The mean-squared diameter $< R^2 >$ and the mean-squared radius of gyration $< S^2 >$ as functions of the chain length N. The solid line on the right indicates the theoretical slope 3/2

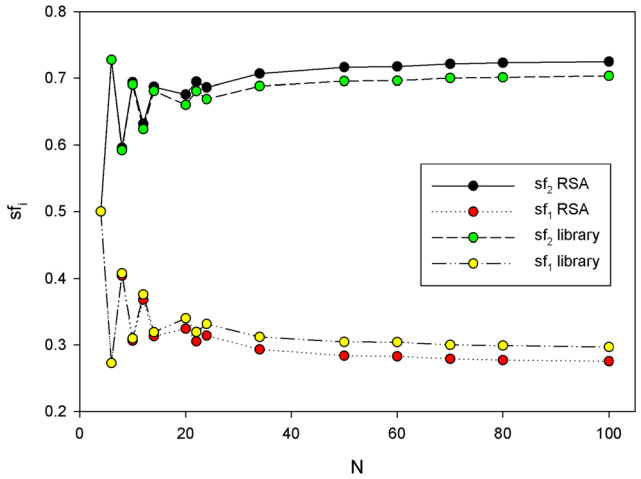

Fig. 9 The shape factors sf_i as functions of the chain length N: the case of the entire library of conformations (library) and only those used successfully in the RSA procedure (RSA)

of ring polymers the principal axis of inertia λ_1^2 and λ_2^2 (with $\lambda_2^2 \geq \lambda_1^2$) were determined from the gyration tensor. These values fulfill the relation $S^2 = {\lambda_1}^2 + {\lambda_2}^2$. The shape of a single chain can be described by two parameters called shape factors:

$$sf_i = \lambda_i^2 / S^2. \quad (6)$$

The other parameter that quantify the shape of a single chain is the asphericity factor δ which can be calculated as [64]:

$$\delta = \frac{\left\langle \left(\lambda_1^2 - \lambda_2^2\right)^2 \right\rangle}{\left\langle \left(\lambda_1^2 + \lambda_2^2\right)^2 \right\rangle}. \quad (7)$$

This parameter takes value δ=1 for a fully extended chain (a one-dimensional rod) and δ=0 for a disk. Figure 9 presents

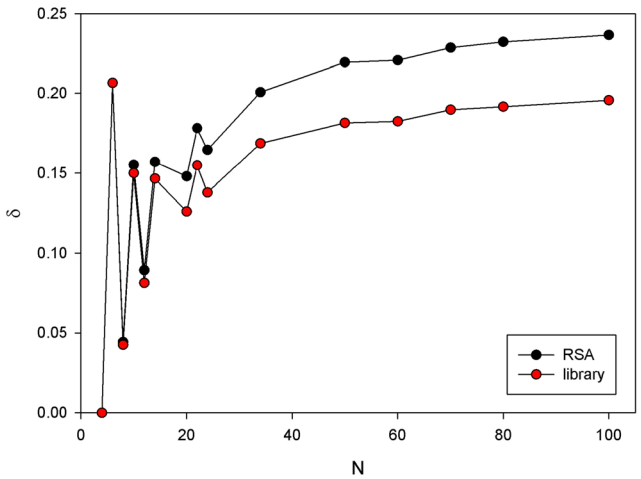

Fig. 10 The asphericity δ as a function of the chain length N: the case of the entire library of conformations (library) and only those used successfully in the RSA procedure (RSA)

shape factors sf_i as functions of the chain length N for polymers put on the substrate. One can observe that for short chains these parameters highly fluctuated which is expected because of the lattice representation. Then, for $N>24$ they stabilize and increase moderately approaching values 0.72 and 0.28. These values are very close to simulation results 0.71 and 0.29 obtained for a similar chain model [14, 16]. The values of shape factors averaged over the entire pool of conformations were added for the sake of comparison to this figure. The comparison of both these pairs of parameters shows that chains that are successfully put on the plane are more prolate than an average single chain from the pool. This behavior can be confirmed by the analysis of the asphericity factor. The influence of the chain length on ashpericity factor δ is shown in Fig. 10. This parameter approaches the value 0.24 for the longest chains under consideration while in the entire pool of conformations it is considerably lower and close to 0.20. Theoretical predictions for unbranched flexible chains without the excluded volume give the value $\delta=2(d+2)/(5d+2)$, where d is the dimensionality of space which in 2D case makes $\delta\approx0.57$ [64]. For two-dimensional rings this parameter was theoretically established as 0.2625 for an infinitely long chain [65]. Monte Carlo simulations of models that were similar to ours (single chains on a square lattice) predicted that the asphericity increases with the chain length approaching $\delta=0.211$ for $N=32$ which is close to that of our library of conformations (what is interesting, chains with the excluded volume were more spherical than random flight chains in two-dimensions) [16]. Thus, one can conclude that in the two-dimensional space cyclic chains are more spherical than flexible linear chains but still considerably prolate.

Conclusions

A simple coarse-grained model of strongly and irreversibly adsorbed (two-dimensional) ring polymer chains was developed. In this model all atomic details were suppressed and chains were represented as cyclic sequences of statistical segments. Positions of polymer segments were limited to vertices of a square lattice and the excluded volume was the only interaction within the system under consideration. Properties of these macromolecular systems were determining by means of the random sequential adsorption simulation technique. The RSA algorithm appeared to be quite efficient for chains of moderate length (no longer than 100 beads for the square lattice model). The percolation threshold was found higher for rings when compared to flexible linear chains because rings were more compact and better packed in the dilute and semidilute solutions. The percolation threshold decreased with the increase of the chain length for both kinds of objects. Contrary to the differences between percolation thresholds the jamming thresholds (the maximum coverage of the substrate) are very similar for both chain architectures. If one considers a cyclic chain together with its interior the jamming threshold behaves similarly to that of regular hard objects like squares but packing abilities of rings are higher.

Acknowledgments The computational part of this work was done using the computer cluster at the Computing Center of the Department of Chemistry, University of Warsaw. This work was supported by the Polish National Science Center grant UMO-2013/09/B/ST5/00093.

References

1. Semlyen JA (2000) Cyclic polymers, 2nd edn. Kluwer, Dordrecht
2. Roovers J (2013) Overview on physical properties of cyclic polymers. In: Tezuka Y (ed) Topological polymer chemistry progress of cyclic polymers in syntheses. Properties and Functions, World Scientific, Singapore
3. McLeish TCB (2008) Nat Mater 7:933–935
4. Kapnistos M, Lang M, Vlassopoulos D, Pyckhout-Hintzen W, Richter D, Cho D, Chang T, Rubinstein M (2008) Nat Mater 7: 997–1002
5. Bielawski CW, Benitez D, Grubbs RH (2022) Science 297:2041–2044
6. Beaucage G, Kulkarni AS (2010) Macromolecules 43:532–537
7. Arrighi V, Gagliardi S, Dagger AC, Semlyen JA, Higgins JS, Shenton MJ (2004) Macromolecules 37:8057–8065
8. Robertson RM, Smith DE (2007) Proc Natl Acad Sci U S A 104: 4824–4837
9. Baldelli Bombelli F, Gambinossi F, Lagi M, Berti D, Caminati G, Brown T, Sciortino F, Norden B, Baglioni P (2008) J Chem Phys B 112:15283–15294
10. Obukhov SP, Rubinstein M, Duke T (1994) Phys Rev Lett 73:1263–1266
11. Zifferer G, Preusser W (2001) Macromol Theory Simul 10:397–407
12. Reiter J (1990) Macromolecules 23:3811–3816
13. Bishop M, Saltiel CJ (1985) J Chem Phys 83:3976–3980
14. Bishop M, Michels JPJ (1985) J Chem Phys 82:1059–1061
15. Bishop M, Michels JPJ (1986) J Chem Phys 84:444–446
16. Bishop M, Slatiel CJ (1986) J Chem Phys 85:6728–6731
17. Suzuki J, Takano A, Matsushita Y (2008) J Chem Phys 129:034903
18. Brown S, Szamel G (1998) J Chem Phys 108:4705–4708
19. Brown S, Szamel G (1998) J Chem Phys 109:6184–6192
20. Kanaeda N, Deguchi T (2008) J Phys A Math Theor 41:145004
21. Brown S, Lenczycki T, Szamel G (2001) Phys Rev E 63:052801
22. Vettorel A, Grossberg AY, Kremer K (2009) Phys Biol 6:025013
23. Tsolou G, Stratikis N, Baig C, Stephanou PS, Mavrantzas VG (2010) Macromolecules 43:10692
24. Suzuki J, Takano A, Deguchi T, Matsushita Y (2009) J Chem Phys 131:144902
25. Eisenriegler E (1993) Polymers near surfaces. World Scientific, Singapore
26. Stauffer D, Aharony A (1994) Introduction to percolation theory. Taylor and Francis, London
27. Żerko S, Polanowski P, Sikorski A (2012) Soft Matter 8:973–979
28. Adamczyk P, Romiszowski P, Sikorski A (2008) J Chem Phys 128: 154911
29. Vigil RD, Ziff RM (1989) J Chem Phys 91:2599–2602
30. Ziff RM, Vigil RD (1990) J Phys A Math Gen 23:5103–5108
31. Vandewalle N, Galam S, Kramer M (2000) Eur Phys J B 14:407–410
32. Kondrat G, Pękalski A (2001) Phys Rev E 63:051108
33. Kondrat G, Pękalski A (2001) Phys Rev E 64:056118
34. Evans JW (1993) Rev Mod Phys 65:1281–1329

35. Tarasevich YY, Cherkasova VA (2007) Eur Phys J B 60:97–100
36. Cieśla M (2013) Phys Rev E 87:052401
37. Romiszowski P, Sikorski A (2013) Comput Methods Sci Technol 19: 115–121
38. Cornette V, Ramirez-Pastor JA, Nieto F (2003) Eur Phys J B 36:391–399
39. Longone P, Centres PM, Ramirez-Pastor AJ (2012) Phys Rev E 85: 011108
40. Matoz-Fernandez DA, Linares DH, Ramirez-Pastor AJ (2012) Eur Phys J B 85:296
41. López LG, Ramirez-Pastor AJ (2012) Langmuir 28:14917–14924
42. Tarasevich YY, Lebovka NI, Laptev VV (2012) Phys Rev E 86: 061116
43. Garboczi EJ, Snyder KA, Douglas JF, Thorpe MF (1995) Phys Rev E 52:819–828
44. Yi YB, Sastry AM (2004) Proc R Soc Lond A 460:2353–2360
45. Li J, Östling M (2013) Phys Rev E 88:012101
46. Chatterjee AP (2014) J Chem Phys 140:304911
47. Becklehimer JB, Pandey RB (1994) J Stat Phys 75:765–771
48. Wang SJ, Pandey RB (1996) Phys Rev Lett 177:1773–1776
49. Kondrat G (2003) J Chem Phys 117:6662–6668
50. Cornette V, Ramirez-Pastor AJ, Nieto F (2003) Eur Phys J B 36:391–399
51. Cornette V, Ramirez-Pastor AJ, Nieto F (2003) Physica A 327:71–75
52. Wang J-S, Pandey RB (1996) Phys Rev Lett 77:1773–1776
53. Lončarević I, Budinski-Petković L, Vrhovac SB, Belić A (2009) Phys Rev E 80:021115
54. Cieśla M, Barbasz J (2013) J Mol Model 19:5423–5427
55. Adamczyk P, Polanowski P, Sikorski A (2009) J Chem Phys 131: 234901
56. De Gennes PG (1979) Scaling concepts in polymer physics. Cornell University Press, Ithaca
57. Sikorski A (2001) Macromol Theory Simul 10:38–45
58. Binder K, Müller M, Baschnagel J (2004) Polymer models on the lattice. In: Kotelyanskii M, Theodorou DN (eds) Simulation methods for polymers. Dekker, NewYork
59. Pawłowska M, Sikorski A (2013) J Mol Model 19:4251–4258
60. Newman MEJ, Ziff RM (2001) Phys Rev E 64:016706
61. Nakamura M (1986) J Phys A Math Gen 19:2345–2351
62. Privman V, Wang JS, Nielaba P (1991) Phys Rev B 43:3366–3372
63. Polanowski P, Jeszka JK, Sikorski A (2014) Macromolecules 47: 4830–4839
64. Rudnick J, Gaspari G (1986) J Phys A Math Gen 19:L191–L193
65. Diehl WH, Eisenriegler E (1989) J Phys A Math Gen 22:L87–L91